

Improving the Sunscreen Properties of TiO₂ through an Understanding of Its Catalytic Properties

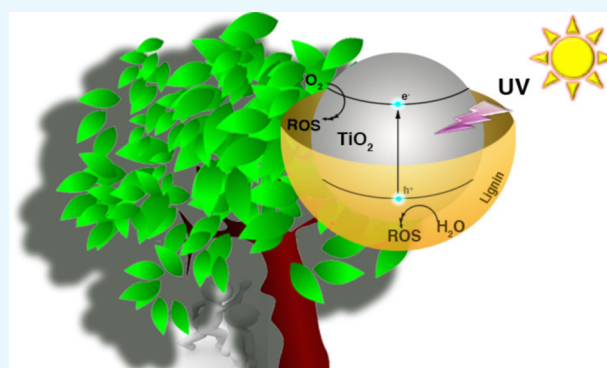
Michela Morsella,^{†,‡} Nicola d'Alessandro,[‡] Anabel E. Lanterna,^{*,†} and Juan C. Scaiano^{*,†}

[†]Department of Chemistry and Biomolecular Sciences and Centre for Catalysis Research and Innovation (CCRI), University of Ottawa, 10 Marie Curie, Ottawa, Ontario K1N 6N5, Canada

[‡]Department of Engineering and Geology, University G. d'Annunzio of Chieti-Pescara, Viale Pindaro, 42, 65127 Pescara, Italy

S Supporting Information

ABSTRACT: The use of particulate titanium dioxide (TiO₂) as an active sunscreen ingredient has raised concerns about potential risks from TiO₂-mediated free radical formation. To date, remediation attempts have concentrated on reducing the yield of free radical generation by TiO₂ upon sunlight exposure. The problem with this approach is that given the band gap in TiO₂, production of radical and the ensuing reactive oxygen species (ROS) is completely normal. Our strategy is based on a nontoxic, biocompatible shell that neutralizes the free radicals by scavenging them with natural antioxidants before they exit the particle. The new lignin@TiO₂ composites preserve the scattering and absorption properties of TiO₂ because the particles retain their nanoscale dimensions as preferred by the cosmetic industry. Although the target properties for photocatalysis and sun-protection applications are opposite, we argue that exactly the same knowledge is required to optimize either one.



INTRODUCTION

Titanium dioxide (TiO₂) is a common ingredient in sunscreens where its loading is frequently 2%–15%, whereas the allowed “loading” of this material is up to 25%, the highest for any sunscreen ingredient. The TiO₂ form mostly employed for these applications is anatase, which is also used in a broad range of applications such as solar cells, photocatalysis, and sterilizing coatings because of its high reactivity.¹ TiO₂ activity relates to the generation of HO• and O₂•− radicals along with other reactive oxygen species (ROS), including H₂O₂.^{2,5} Given these catalytic applications, it is hardly surprising that the use of TiO₂ in sunscreens has been tainted by reports of enzyme inactivation and potential damage to biomolecules, to the extent that its use in sunscreens has been described as “a societal experiment.”⁴ Although there are a few indications that noncoated TiO₂ nanoparticles (NPs)⁵ do not penetrate either healthy or damaged skin, some authors emphasize that further studies for the safety evaluation of the TiO₂ NPs in sunscreens must be undertaken to simulate real-world conditions, particularly in sunburned skin and under UV exposure.⁶ The same controversial opinions are reported in different studies that suggest the penetration⁷ or not⁸ of zinc oxide and its dangerous disposal.⁹ Moreover, whether or not TiO₂ penetrates the skin, there is evidence that hydrogen peroxide and singlet oxygen,¹⁰ two of its products of sunlight exposure, do. Beyond the evaluation of titania toxicity on its potential adverse health consequences, it is clear that any strategy that reduces the ability of TiO₂ to generate and release ROS, while preserving or

enhancing its desirable properties (i.e., light absorption and scattering), would ease some of the concerns that society as a whole and cosmetic manufacturing in particular may have. Whereas eliminating the reactivity of TiO₂ under illumination may prove to be quite challenging, an alternative strategy that we use here is to scavenge ROS and other species that may be formed before they diffuse away from TiO₂ and cause damage to either biomolecules or other important sunscreen ingredients. Our approach is different from the usual modifications of TiO₂ using SiO₂ or Al₂O₃¹¹ or from the known attenuation of radical generation upon encapsulation in large-pore zeolites.¹² SiO₂ or Al₂O₃ shells are designed to increase the energy band gap of TiO₂ to make the formation of ROS more energetic (less favored). Here, we do not attempt to reduce the generation of ROS through band-gap alteration but to prevent them from being released into the surrounding media. For this purpose, we decided to look for an antioxidant organic shell.¹³ We demonstrate here that by using lignin to construct a thin shell around TiO₂ particles we can achieve this goal.

Lignin is a natural, heterogeneous, and cross-linked phenolic polymer.¹⁴ It is the second most abundant biopolymer on earth, mainly obtained as a waste product in the wood-pulp and sugarcane milling industries. Additionally, lignin is also environment-friendly, biocompatible, biodegradable, and harm-

Received: August 8, 2016

Accepted: September 13, 2016

Published: September 23, 2016

less for human health.¹⁵ As mentioned above, the ROS photogenerated on the surface of TiO₂ can diffuse and thus react with the surrounding medium, either biostructures or other organic ingredients of the sunscreen formulations.¹⁶ Recent studies have reported that lignin is a good UV-absorbent coating¹⁷ and is able to contribute as a sunblock, protecting organic filters from photodegradation.¹⁸

The new hybrid material developed in this work takes advantage of the free radical scavenging and antioxidant properties of lignin,¹³ which is effectively used as a sacrificial scavenger for the ROS anticipated from TiO₂. An earlier publication demonstrated that when TiO₂ is embedded in a lignin matrix, the free radical activity of TiO₂ is diminished, thus providing a good indication that the lignin matrix can be an effective scavenger for these radicals.¹⁹ Here, we managed to shield TiO₂ NPs using a very thin shell of lignin, a nontoxic and extremely versatile product. Thus, a thin coating, rather than a thick matrix, can provide enough protection while TiO₂ retains the nanostructured features that have made it a broadly employed material in sun protection and cosmetics.

To evaluate the effect of a lignin shell on TiO₂ reactivity and its use as a potential ingredient in sunscreens and cosmetics, several types of experiments were performed. Here, we present the synthesis and characterization methods of different lignin@TiO₂ hybrids. The reduced photocatalytic activity of the modified TiO₂ particles using the photo-oxidation of 2-propanol to acetone as a test reaction¹⁹ and the concomitant decrease in the TiO₂-mediated photodamage to enzymes are also described. Additionally, the photoprotection of other sunscreen active ingredients by the lignin-modified TiO₂ particles is shown.

EXPERIMENTAL SECTION

Synthesis of Particles. Briefly, 10 (mg) (or 100 mg) of lignin was solubilized in 5 mL of solvent [water or tetrahydrofuran (THF), according to the solubility properties of the corresponding lignin] and placed together with 10 mg of TiO₂. The mixture was kept in the dark overnight and then subjected to UVA (368 nm LED) irradiation for 2 h under vigorous stirring. The slurry was separated by centrifugation and washed three times. The resulting particles were dried at 100–120 °C for at least 1 h; this should eliminate any residual THF (bp 65 °C). The particles were characterized using attenuated total reflection—infra-red (ATR-IR) spectroscopy, diffuse reflectance (DR) spectroscopy, transmission electron microscopy (TEM), and thermogravimetric analysis (TGA).

Photocatalytic Oxidation of 2-Propanol. The photo-activity of the NPs was observed using the photo-oxidation of 2-propanol to acetone as a reference reaction as previously reported.¹⁹ The reaction was carried out at 35–38 °C under combined UVA–UVB irradiation (10 UVA lamps and 4 UVB lamps). Control experiments under dark conditions were also performed (TiO₂, lignin, and lignin@TiO₂) showing no reaction. The conversion of 2-propanol in an aqueous solution (5 mM) under stirring was evaluated in the presence of TiO₂ and several lignin@TiO₂ NPs. For this, 1 mL aliquots of particles were used to reach a final concentration of 0.4 mg/mL in 5 mL, and the sample was collected at 1 h intervals for 5 h. Each aliquot was centrifuged at 7000 rpm, 20 °C, for 10 min, and 800 μ L of the supernatant was used to record the ¹H NMR spectrum using the water suppression sequence, with the presaturation signal centered at 4.706 ppm (proton signal of H₂O) in the presence of 3-(trimethylsilyl)-2,2,3,3-tetradeutero

propionic acid (sodium salt) (TMSP) in D₂O as the external standard to analyze the degradation of 2-propanol over irradiation time using a calibration curve previously fitted.

Enzyme Inactivation: TiO₂-Mediated Photodamage. Alkaline phosphatase (ALP) from the bovine intestinal mucosa (0.02 mg/mL) solution and particle suspension (0.25 mg/mL) were prepared in a cold buffer (1.0 M diethanolamine with 0.50 mM magnesium chloride) of pH 9.8 at 37 °C. The substrate solution of *p*-nitro phenylphosphate (PNPP) was prepared in water with a concentration of 0.5 mM. The enzyme was subjected to UVA irradiation for 30 min in the absence and in the presence of 50 μ g/mL TiO₂ or lignin@TiO₂ under stirring. Then, the suspensions were centrifuged at 11 000 rpm for 15 min at 0 °C. Control reactions under dark conditions were also performed. The enzymatic assay was performed in a 96-well plate using the following final concentrations: [PNPP] = 25 μ M and [ALP] = 1.5 μ g/mL. The enzyme activity was followed by monitoring the absorbance changes at 405 nm, where the dephosphorylated product has a maximum absorption.

Compatibility with Avobenzone. An avobenzone aqueous solution (24 μ M) was prepared in a 1 mM Brij-10 solution (<0.04% 2-propanol). The mixture was sonicated for 3 h and stored in the dark overnight. The reaction was carried out using 8 mL of this solution in a quartz test tube placed in a photoreactor equipped with 10 UVA lamps and 4 UVB lamps under stirring. TiO₂ and several lignin@TiO₂ NPs were tested using three different avobenzone/particle ratios: 1/13, 1/41, and 1/82 (w/w). Samples (1 mL) were collected at 1 h intervals for 4 h and centrifuged at 7000 rpm, 20 °C for 10 min. Each aliquot was analyzed using UV spectroscopy, recording absorbance at 362 nm.

RESULTS AND DISCUSSION

Synthesis and Characterization. Different types of lignin (see Supporting Information) were used for the synthesis of the new material, ranging from water-soluble lignin to lignin that can only be solubilized in organic solvents (Table 1). The

Table 1. Different Types of Lignin Used for TiO₂ Encapsulation

name	type of lignin	solubility
L1	kraft lignin	organic
L2	organosolv lignin	organic
L3	low sulfonate content (LSC)	aqueous
L4	sodium lignin	aqueous
L5	sodium lignin without sugars	aqueous
L6	alkali lignin	aqueous

particles can be easily synthesized under very mild conditions taking advantage of the photocatalytic activity of TiO₂.³ Upon UVA irradiation of a mixture of lignin solution (organic or aqueous solution depending on the type of lignin used) in the presence of TiO₂, lignin can be cross-linked over the particle surface (because of the light-induced ROS generation) and can lead to lignin-coated TiO₂ NPs within a couple of hours. Here, the photocatalytic activity of TiO₂ generates radical species that can cross-link the polymeric moieties of lignin on the surface of TiO₂ thanks to UV radiation as suggested by Mukherjee et al.²⁰

Figures 1 and 2 show the functionalization of TiO₂ using L1. Similar results were found for the other types of lignin used (Figures S1 and S2). According to the IR spectrum of TiO₂, the band at 3400 cm⁻¹ is due to the OH stretching, whereas at

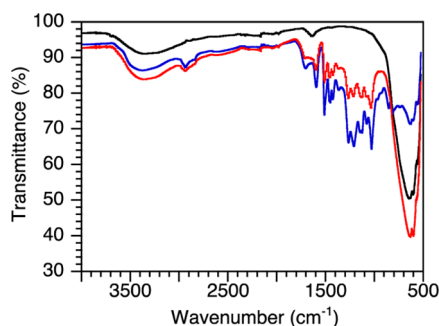


Figure 1. ATR-IR spectra of TiO₂ (black), L1 (blue), and L1@TiO₂ (red).

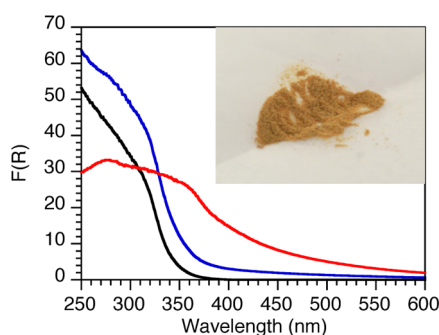


Figure 2. DR spectra of TiO₂ (black), L1 (red), and L1@TiO₂ (blue). Inset: picture showing the color of a sample powder.

1630 cm⁻¹ we can observe OH bending vibrations. Between 1000 and 400 cm⁻¹, the broad band is related to the Ti–O–Ti stretching bonds. On the other hand, the characteristic peaks of lignin are at 2900 cm⁻¹ for sp³ C–H stretching, 1600 cm⁻¹ for C=O stretching, and below 1500 cm⁻¹ for the aromatic ring bending. In general, all particles clearly show signals corresponding to both TiO₂ and lignin. The DR spectra in Figure 2 show that the particles can slightly extend the absorption of TiO₂ to the visible light region (normally below 400 nm) because of the presence of lignin. Note that the thin lignin coating makes these compositions cosmetically acceptable not only in terms of light absorption and scattering but also in terms of the visible color and appearance (inset of Figure 2). In fact, lignin@TiO₂ NPs show a very light tint suitable for skincare formulations. Additionally, because the particles are insoluble in water, they are effectively waterproof.

The high-resolution transmission electron microscopy (HR-TEM) image in Figure 3 suggests that an organic shell surrounds the TiO₂ particles and, more importantly, that the

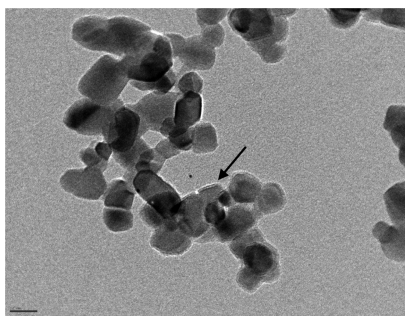


Figure 3. TEM image of L3@TiO₂ showing an organic shell surrounding the inorganic particle (arrow). The scale bar is 20 nm.

particles retain their nanometric size (≤ 50 nm). Table 2 shows the amount of lignin found on each particle using TGA. The

Table 2. Weight Percentage of Lignin in Each Particle Found after TGA

particle	lignin (wt %) ^a	shell thickness (nm) ^b
L1@TiO ₂	43	9.5
	13 ^c	3.6
L2@TiO ₂	18	4.7
	8 ^c	2.3
L3@TiO ₂	9	2.6
	5 ^c	1.5
L4@TiO ₂	8	2.3
L5@TiO ₂	6	1.8
L6@TiO ₂	3	0.9

^aSynthesized using 100 mg of lignin unless otherwise indicated. ^bShell thickness calculated with a density of 3.8 g mL⁻¹ for anatase (10 mg) and assuming a 50 nm particle size. ^cSynthesis using 10 mg of lignin.

organosoluble lignins generate particles with higher loadings, presumably because of the presence of more conjugated structures in those types of lignin that can interact better with the free radicals generated by TiO₂.²¹ In commercial formulations, the presence of dispersants will normally reduce aggregation.

The stability of the particles in an aqueous solution upon UVA–UVB irradiation was monitored using UV spectroscopy, following the absorption at the wavelength of maximum absorption of the corresponding lignin. Thus, the absorbance due to leached or degraded lignin can be measured in the supernatant of the mixture after 2 h of irradiation. Figure 4

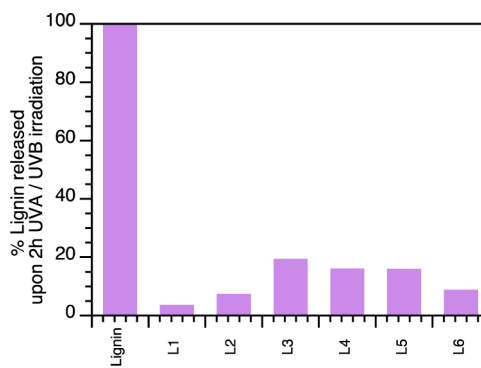


Figure 4. Percentage of lignin released (or degraded) upon UVA–UVB irradiation for 2 h. The plot assumes that the absorption coefficient of lignin is constant, that is, insensitive to exposure or release. Data reproducible within $\pm 5\%$.

shows that the particles exhibit great stability under UVA–UVB exposure (Figure S4). As expected, the percentage of organosoluble lignins (L1 and L2) released was lower compared with water-soluble lignins.

Photocatalytic Oxidation of 2-Propanol. We evaluated the photocatalytic activity of TiO₂ by using the well-known oxidation of alcohols to ketones as a test reaction.³ Here, we used an established methodology¹⁹ to evaluate the inhibition of the photocatalytic activity of TiO₂ when modified with lignin. The conversion of 2-propanol in an aqueous solution was evaluated in the presence of TiO₂ and several lignin@TiO₂ NPs at 35–38 °C under combined UVA–UVB irradiation. Control

experiments under dark conditions were also performed. Figure 5 shows the photocatalytic activities exhibited by the different

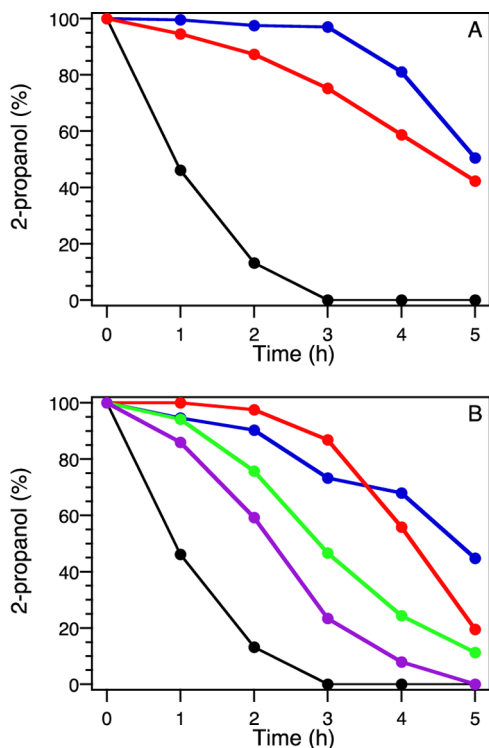


Figure 5. Percentage of 2-propanol remaining upon UVA–UVB irradiation in the presence of different particles. (A) TiO₂ (black), L1@TiO₂ (blue), and L2@TiO₂ (red). (B) TiO₂ (black), L3@TiO₂ (blue), L4@TiO₂ (red), L5@TiO₂ (green), and L6@TiO₂ (violet).

lignin@TiO₂ composites compared to those of the pristine TiO₂. Notice that 2-propanol is totally consumed after 3 h of irradiation in the presence of TiO₂, but different percentages of alcohol still remain when treated with lignin-modified TiO₂. Thus, although the strategy used to synthesize the lignin@TiO₂ is based on the photocatalytic activity of TiO₂, the new composites exhibit the capacity to inhibit free radical reactions. This concept underlies the basic premise of this work: *understanding catalysis helps design sunscreens*; that is, although the objectives of the materials designed are opposite, the knowledge requirements are much the same. Indeed, the particles showing the worst photocatalytic activity were chosen as the best potential sunscreens. From Figure 5, L1@TiO₂, L2@TiO₂, and L3@TiO₂ were selected for further examination, although L4@TiO₂ also shows excellent performance.

Enzyme Inhibition: TiO₂-Mediated Photodamage. In addition to the decrease in the photocatalytic activity demonstrated for the lignin-modified TiO₂, the new composites also need to be innocuous for future topical uses. To evaluate this, we tested the enzymatic activity of ALP after exposure to different lignin@TiO₂ NPs. It is well known that bare TiO₂ can act as an enzyme inhibitor through a process not yet fully understood²² but accelerated by UV light and most likely radical-mediated.²³ Hence, we carried out an enzymatic assay using ALP pretreated with different particles under light exposure and under dark conditions. Equation 1 shows the dephosphorylation reaction used to determine the enzymatic activity, simply by monitoring the formation of *p*-nitrophenol using UV–vis spectroscopy.

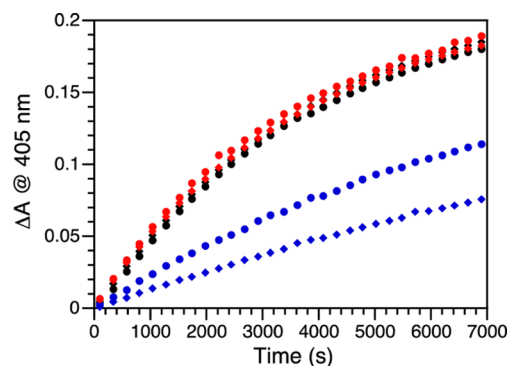
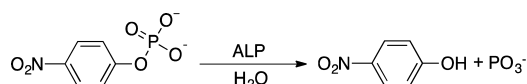


Figure 6. Kinetic slopes of the enzymatic activity of ALP acquired at 405 nm for the dephosphorylation of PNNP. Traces recorded after the enzyme pretreatment in the absence of particles (black) and in the presence of TiO₂ (blue) or L1@TiO₂ (red). Circles represent dark conditions, and diamonds represent UVA irradiation for 30 min.

The kinetic traces (Figure 6) acquired at 405 nm for the formation of *p*-nitrophenol are a reflection of the activity of the enzyme. Each curve is then fitted with the expression

$$A_{405\text{nm}} = a + bt + ct^2 \quad (2)$$

where A is the absorbance and t is the time. The coefficients a , b , and c are fitting parameters. The derivative of this expression with respect to t is given by

$$\frac{dA}{dt} = b + ct \quad (3)$$

which at $t = 0$ corresponds to b . That is, the first coefficient (b) of the quadratic fit is the calculated initial slope. These slopes have been used as a measure of the initial enzymatic activity.

Figure 7 shows the initial rates calculated for the enzymatic activity of ALP after treatment with TiO₂ and lignin@TiO₂ particles. As expected, TiO₂ can decrease the enzymatic activity simply by contact (dark conditions), but exposure to UV light can exacerbate this inhibition. Coating the TiO₂ NPs with

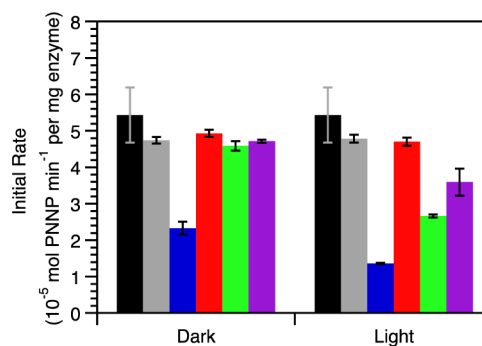


Figure 7. Initial rates calculated for the enzymatic activity of ALP in the dark and upon UVA irradiation in the absence (black/gray) and in the presence of TiO₂ (blue), L1@TiO₂ (red), L2@TiO₂ (green), and L3@TiO₂ (violet).

lignin prevents the enzyme inactivation even under light irradiation. These results indicate clearly that the UVA irradiation does not affect the enzyme and, more importantly, lignin@TiO₂ NPs are completely innocuous for the enzymatic activity under dark conditions. The TiO₂-mediated photo-damage under UVA irradiation is highly reduced in the presence of lignin, and the L1@TiO₂ composite shows no enzyme inactivation. Clearly, the changes that prevent alcohol photo-oxidation also inhibit enzyme inactivation.

Compatibility with Avobenzone. Finally, to determine the compatibility of these new particles with other sunscreen ingredients, the photoprotection of avobenzone was tested. Avobenzone is a widely used UVA protector, largely present in an enol form that photodegrades readily upon UVA–UVB exposure through a mechanism involving a photoinduced enol–keto transformation.²⁴ Other sunscreens can stabilize avobenzone either by competitive light absorption (or scattering) or by quenching its excited states.²⁵ Given the ubiquitous use of avobenzone, we felt that it was important to establish its compatibility with the new hybrid materials to evaluate as to what extent they could be involved in the process of photodegradation or photoprotection of avobenzone.

Figure 8 shows the photodegradation of avobenzone after exposure to 2 and 4 h of UVA–UVB irradiation using different amounts of particles. Notice that at lower particle concentrations, TiO₂ can act as a photoprotector (graphs A and B), although when the TiO₂ particle concentration is increased this ability is lost. By contrast, the new particles retain the photoprotection ability even at high TiO₂ concentrations. These results show that the new particles not only preserve the photoprotection properties that TiO₂ provides to avobenzone (graph A) but also prevent the photodegradation of avobenzone when the amount of TiO₂ added generates a high concentration of ROS (graph C). This opens the opportunity to increase the amount of TiO₂ particles in formulations preserving the integrity of other organic active ingredients.

CONCLUSIONS

Regardless of its great light absorption and scattering properties, there are some health concerns about the use of TiO₂ because of its intrinsic photocatalytic properties. Thus, TiO₂ can generate ROS in the presence of water upon UVA irradiation. The *in vitro* studies reported here suggest that TiO₂ particles can be modified to decrease their photocatalytic activity, while retaining the absorption and scattering properties desirable for sunscreens and cosmetic applications. Thus, the potential risks from TiO₂-mediated free radical generation can be mitigated by shielding the particles with a good antioxidant; in our case, we use a nontoxic, biocompatible lignin shell that scavenges the free radicals before they can exit the new TiO₂–lignin composites, preserving the scattering and the UV absorption characteristics. For this purpose, we demonstrated that this stable lignin@TiO₂ composite plays an important role in reducing the photocatalytic activity of TiO₂ in chemical and enzymatic reactions, improving the photoprotection of the other ingredients even when they are present at high concentrations. To the best of our knowledge, from the cosmetic and public perception point of view, we believe that the particles described here, showing a nanometric size and a very light color, are promising candidates as ingredients in skincare formulations, especially for sunscreens, given that they are nontoxic and waterproof. Additionally, our approach

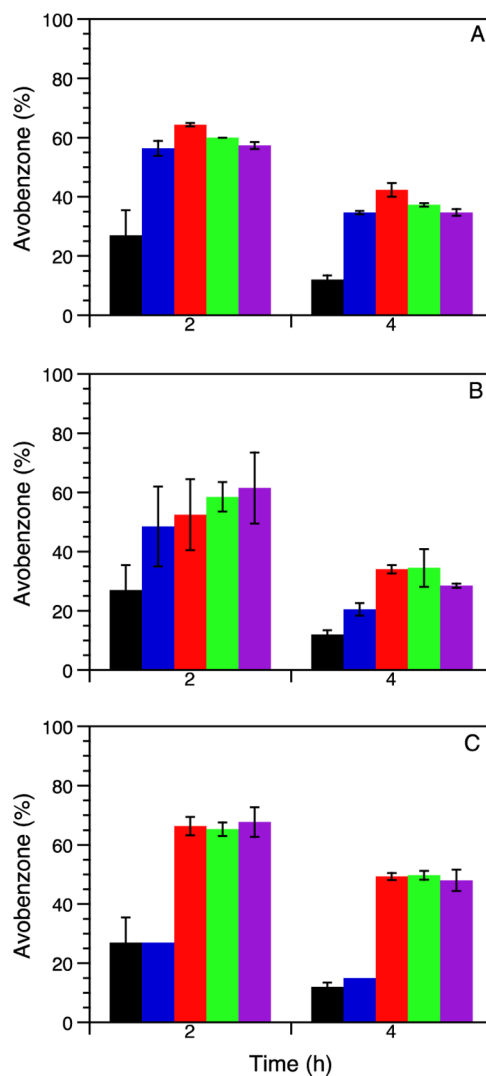


Figure 8. Avobenzone photodegradation using different amount of particles: (A) 0.01, (B) 0.03, and (C) 0.06 wt %. Percentage of avobenzone remaining upon UVA–UVB irradiation in the absence (black) and in the presence of TiO₂ (blue), L1@TiO₂ (red), L2@TiO₂ (green), and L3@TiO₂ (violet).

regarding the use of a safe and extremely versatile material, mainly a byproduct of the paper industry, also contributes to the development of eco-friendly processes for the cosmetic industry.

ASSOCIATED CONTENT

Supporting Information

The Supporting Information is available free of charge on the ACS Publications website at DOI: 10.1021/acsomega.6b00177.

Details of the materials used, instrumentation and experimental procedures, IR and DR spectra, and TEM images (PDF)

AUTHOR INFORMATION

Corresponding Authors

*E-mail: Anabel.lanterna@icloud.com (A.E.L.).

*E-mail: titoscaiano@mac.com (J.C.S.).

Author Contributions

All authors have given approval to the final version of the manuscript.

Notes

The authors declare no competing financial interest.

ACKNOWLEDGMENTS

The authors acknowledge the Natural Sciences and Engineering Council of Canada (NSERC), the Canada Foundation for Innovation (CFI), and the Canada Research Chairs Program (CRC) for the support for this research. M.M. is a grateful recipient of a fellowship from Erasmus Nova Domus program.

REFERENCES

- (1) (a) Hoffmann, N. *Aust. J. Chem.* **2015**, *68*, 1621–1639. (b) Nakata, K.; Fujishima, A. *J. Photochem. Photobiol., C* **2012**, *13*, 169–189. (c) Banerjee, S.; Dionysiou, D. D.; Pillai, S. C. *Appl. Catal., B* **2015**, *176*, 396–428. (d) Schneider, J.; Matsuoka, M.; Takeuchi, M.; Zhang, J.; Horiuchi, Y.; Anpo, M.; Bahnemann, D. W. *Chem. Rev.* **2014**, *114*, 9919–9986. (e) Roose, B.; Pathak, S.; Steiner, U. *Chem. Soc. Rev.* **2015**, *44*, 8326–8349.
- (2) (a) Augugliaro, V.; Bellardita, M.; Loddo, V.; Palmisano, G.; Palmisano, L.; Yurdakal, S. *J. Photochem. Photobiol., C* **2012**, *13*, 224–245. (b) Fox, M. A.; Lindig, B.; Chen, C. C. *J. Am. Chem. Soc.* **1982**, *104*, 5828–5829.
- (3) Fox, M. A.; Dulay, M. T. *Chem. Rev.* **1993**, *93*, 341–357.
- (4) Jacobs, J. F.; van de Poel, I.; Osseweijer, P. *Nanoethics* **2010**, *4*, 103–113.
- (5) (a) Campbell, C. S. J.; Contreras-Rojas, L. R.; Delgado-Charro, M. B.; Guy, R. H. *J. Controlled Release* **2012**, *162*, 201–207. (b) Shi, H.; Magaye, R.; Castranova, V.; Zhao, J. *Part. Fibre Toxicol.* **2013**, *10*, 15. (c) Filipe, P.; Silva, J. N.; Silva, R.; de Castro, J. L. C.; Gomes, M. M.; Alves, L. C.; Santus, R.; Pinheiro, T. *Skin Pharmacol. Physiol.* **2009**, *22*, 266–275. (d) Senzui, M.; Tamura, T.; Miura, K.; Ikarashi, Y.; Watanabe, Y.; Fujii, M. *J. Toxicol. Sci.* **2010**, *35*, 107–113.
- (6) Newman, M. D.; Stotland, M.; Ellis, J. I. *J. Am. Acad. Dermatol.* **2009**, *61*, 685–692.
- (7) Gulson, B.; McCall, M.; Korsch, M.; Gomez, L.; Casey, P.; Oytam, Y.; Taylor, A.; McCulloch, M.; Trotter, J.; Kinsley, L.; Greenoak, G. *Toxicol. Sci.* **2010**, *118*, 140–149.
- (8) Cross, S. E.; Innes, B.; Roberts, M. S.; Tsuzuki, T.; Robertson, T. A.; McCormick, P. *Skin Pharmacol. Physiol.* **2007**, *20*, 148–154.
- (9) Deng, X.; Luan, Q.; Chen, W.; Wang, Y.; Wu, M.; Zhang, H.; Jiao, Z. *Nanotechnology* **2009**, *20*, 115101.
- (10) (a) Poljsak, B.; Dahmane, R. *Dermatol. Res. Pract.* **2012**, *2012*, 135206. (b) Pillai, S.; Oresajo, C.; Hayward, J. *Int. J. Cosmet. Sci.* **2005**, *27*, 17–34.
- (11) (a) Carlotti, M. E.; Ugazio, E.; Sapino, S.; Fenoglio, I.; Greco, G.; Fubini, B. *Free Radical Res.* **2009**, *43*, 312–322. (b) Tiano, L.; Armeni, T.; Venditti, E.; Barucca, G.; Mincarelli, L.; Damiani, E. *Free Radicals Biol. Med.* **2010**, *49*, 408–415.
- (12) Fox, M. A.; Doan, K. E.; Dulay, M. T. *Res. Chem. Intermed.* **1994**, *20*, 711–721.
- (13) Ponomarenko, J.; Lauberts, M.; Dizhbite, T.; Lauberte, L.; Jurkane, V.; Telysheva, G. *Holzforchung* **2015**, *69*, 795–805.
- (14) Constant, S.; Wienk, H. L. J.; Frissen, A. E.; de Peinder, P.; Boelens, R.; van Es, D. S.; Grisel, R. J. H.; Weckhuysen, B. M.; Huijgen, W. J. J.; Gosselink, R. J. A.; Bruijninx, P. C. A. *Green Chem.* **2016**, *18*, 2651–2665.
- (15) (a) Ge, Y.; Wei, Q.; Li, Z. *BioResources* **2014**, *9*, 6699–6706. (b) Thakur, V. K.; Thakur, M. K.; Raghavan, P.; Kessler, M. R. *ACS Sustainable Chem. Eng.* **2014**, *2*, 1072–1092. (c) Ugartondo, V.; Mitjans, M.; Touriño, S.; Torres, J. L.; Vinardell, M. P. *Chem. Res. Toxicol.* **2007**, *20*, 1543–1548.
- (16) (a) Kansal, S. K.; Singh, M.; Sud, D. *J. Hazard. Mater.* **2008**, *153*, 412–417. (b) Ksibi, M.; Amor, S. B.; Cherif, S.; Elaloui, E.; Houas, A.; Elaloui, M. *J. Photochem. Photobiol., A* **2003**, *154*, 211–218.
- (17) Hambarzumyan, A.; Foulon, L.; Chabbert, B.; Aguié-Béghin, V. *Biomacromolecules* **2012**, *13*, 4081–4088.
- (18) Qian, Y.; Qiu, X.; Zhu, S. *Green Chem.* **2015**, *17*, 320–324.
- (19) Morsella, M.; Giammatteo, M.; Arrizza, L.; Tonucci, L.; Bressan, M.; d'Alessandro, N. *RSC Adv.* **2015**, *5*, 57453–57461.
- (20) Mukherjee, D.; Barghi, S.; Ray, A. *Processes* **2013**, *2*, 12–23.
- (21) Qian, Y.; Qiu, X.; Zhu, S. *ACS Sustainable Chem. Eng.* **2016**, *4*, 4029–4035.
- (22) (a) Fenoglio, I.; Greco, G.; Livraghi, S.; Fubini, B. *Chem.—Eur. J.* **2009**, *15*, 4614–4621. (b) Hancock-Chen, T.; Scaiano, J. C. *J. Photochem. Photobiol., B* **2000**, *57*, 193–196. (c) Wu, Z.; Zhang, B.; Yan, B. *Int. J. Mol. Sci.* **2009**, *10*, 4198–4209.
- (23) Schug, H.; Isaacson, C. W.; Sigg, L.; Ammann, A. A.; Schirmer, K. *Environ. Sci. Technol.* **2014**, *48*, 11620–11628.
- (24) (a) Aliaga, C.; Stuart, D. R.; Aspée, A.; Scaiano, J. C. *Org. Lett.* **2005**, *7*, 3665–3668. (b) Andrae, I.; Bringham, A.; Böhm, F.; Gonzenbach, H.; Hill, T.; Mulroy, L.; Truscott, T. G. *J. Photochem. Photobiol., B* **1997**, *37*, 147–150.
- (25) Bonda, C. *Cosm. Toiletries* **2008**, *123*, 49–60.